

CONSOLIDATION OF LUBRICATED FERROMAGNETIC POWDER MIXES FOR AC SOFT MAGNETIC APPLICATIONS

L.P. Lefebvre, C. Gélinas* and P.E. Mongeon

**Industrial Materials Institute/National Research Council Canada,
75 de Mortagne, Boucherville, Québec, Canada J4B 6Y4**

*** Quebec Metal Powders Limited,
1655 Marie Victorin, Tracy, Québec, Canada, J3R 4R4**

ABSTRACT

Soft magnetic composite powders can be used in AC applications as an alternative to steel laminations. As opposed to laminates, parts consolidated using powder metallurgy techniques have isotropic magnetic and thermal properties. Also, complex geometries can be obtained in a reduced number of manufacturing steps using these near-net-shape manufacturing techniques. In order to meet specific application requirements, many variants of ferromagnetic materials have been developed, which sometimes require adjustments in the consolidation process. Recently, a press-ready mix was developed in order to ease the consolidation using conventional P/M compaction techniques.

Since properties of ferromagnetic parts greatly depend on their density, it is important to determine this density-property relationship. In this paper, the density, resistivity, transverse rupture strength and magnetic properties of a ferromagnetic material consolidated at different compacting pressures are presented. An evaluation of this material pressed into stator segments on an industrial press is also presented and discussed.

1. INTRODUCTION

Soft magnetic components can be produced to near-net-shape using powder metallurgy (P/M) techniques. Depending on the application, different materials and processing conditions may be selected. For instance, in DC magnetic applications, the permeability and induction are usually the properties to maximize. Thus, the purity of the base powder, the type of alloying element (P, Si, Ni, ...), the density and sintering conditions are adjusted to optimize these properties. In AC

applications, the ferromagnetic particles must be electrically insulated from each other in order to reduce the eddy-current losses in the components. The dielectric materials generally used in these composites do not withstand high temperature and these components are usually not sintered. For these applications, the purity of the base powder, the quality of the interparticular insulation or resistivity, the density and post-treatment conditions (curing, low temperature treatments, ...) are key processing parameters.

The application frequency as well as the part cross section (perpendicular to the magnetic flux path) are important considerations when selecting the material and processing conditions that optimize the component properties for a given application [1]. For example, permeability is inversely proportional to the dielectric content while the electrical resistivity increases with its content [2]. For that purpose, the dielectric content is selected to maximize the permeability without sacrificing too much the resistivity in order to maintain low eddy-currents and complete magnetization of the part at the operating frequency. Optimization of composite materials must also take into account the subsequent steps involved in P/M manufacturing such as the powder handling, compaction, ejection and post-compaction treatment. For instance, the size or complexity of the parts to be pressed may be a limiting factor in the achievement of the desired density. The compressibility and the ejection behavior of the composite powder are both important parameters in P/M part manufacturing and may, in some cases, limit the obtainable mechanical and magnetic properties.

It is with all these considerations in mind, related to both optimal properties and component fabrication, that a new ferromagnetic material formulation was studied in the laboratory as well as on an industrial press. This composite powder is a press-ready mix intended for AC magnetic applications at low frequency (50-60 Hz). The density, resistivity, mechanical and magnetic properties achieved at different compacting pressures were evaluated. The compaction and ejection characteristics as well as the stability of the compaction process were also evaluated during the production of stator segments for an electric DC motor.

2. EXPERIMENTAL PROCEDURE

The composite powder used in this study is based on a high purity water-atomized iron powder (ATOMET 1001HP manufactured by QMP) and a lubricating dielectric powder. Transverse rupture bars (3.175 x 1.27 x 0.635 cm) and rings (OD = 5.26 cm, ID = 4.34 cm, h = 0.635 cm) were pressed at 6.80, 7.00 and 7.20 g/cm³ in a double action floating-die at 55°C. After compaction, the specimens were heat treated in a tube furnace at 325°C in air for 30 minutes. Some of the treated specimens were afterwards impregnated with an epoxy resin under vacuum and cured at 75°C to cross-link the resin.

The density, transverse rupture strength (TRS) and electrical resistivity were measured on the rectangular bars. Transverse rupture tests were made according to MPIF Standard 41. The electrical resistivity was evaluated using a four-point contact probe and a micro-ohmmeter adapted for this application. Five readings were taken on the top and bottom faces of each bar and averaged. The compacting and ejection characteristics of the powder mix were evaluated using an instrumented cylindrical die operating in single action mode. The applied and transmitted pressures through the compact were measured by two independent load cells. The measurements of the displacement of the lower punch were converted to give the average in-die density, assuming that the H13 steel die was rigid and not deformed during the tests. In this study, cylinders having 9.5 mm diameter and 8 mm thickness were pressed at 45°C.

The magnetic properties of the material were evaluated on two rings for every experimental condition. The DC properties were determined at an applied field of 11,940 A/m (150 Oe) and the AC properties determined at 60 Hz and 400 Hz, at magnetizations up to 1 Tesla.

In the second part of the study, the powder mix was compacted into stator segments on an industrial 150 ton mechanical press at a rate of 5 parts per minute. One of these segments is shown in Figure 1. The stator segments are part of a DC electric motor used in an electric bicycle. The stator shape is the result of an optimized design that integrates the beneficial attributes of both the material (isotropic properties) and the compaction process (near-net-shape process). During these production trials, the compaction and ejection characteristics of the powder mix, the effect of compaction pressure and stator segment thickness on the compaction/ejection characteristics as well as the stability of the compaction process were evaluated.



Figure 1 : Stator segment compacted from the press-ready powder mix used in this study.

3. RESULTS

3.1 Material properties: effect of density.

The apparent density and Hall flow rate of the press-ready composite powder were 3.00 g/cm³ and 29 s/50g respectively. The compressibility curve, as measured on transverse rupture bars, is given in Figure 2. A green density of about 7.20 g/cm³ was obtained at a compacting pressure of 620 MPa (45 tsi). The high compressibility of this composite powder is attributed to the high-purity of the water-atomized iron powder and to the good lubricating properties of the dielectric material. A more detailed analysis of the material compaction and ejection behavior of this powder was carried out using an instrumented cylindrical die. The compressibility and ejection curves measured on 9.5 mm diameter by 8 mm thick cylinders are given in Figure 3.

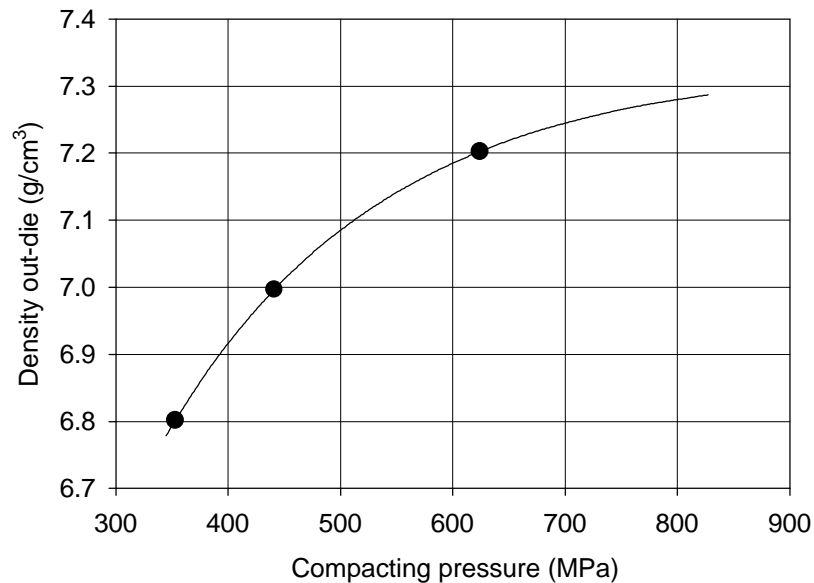
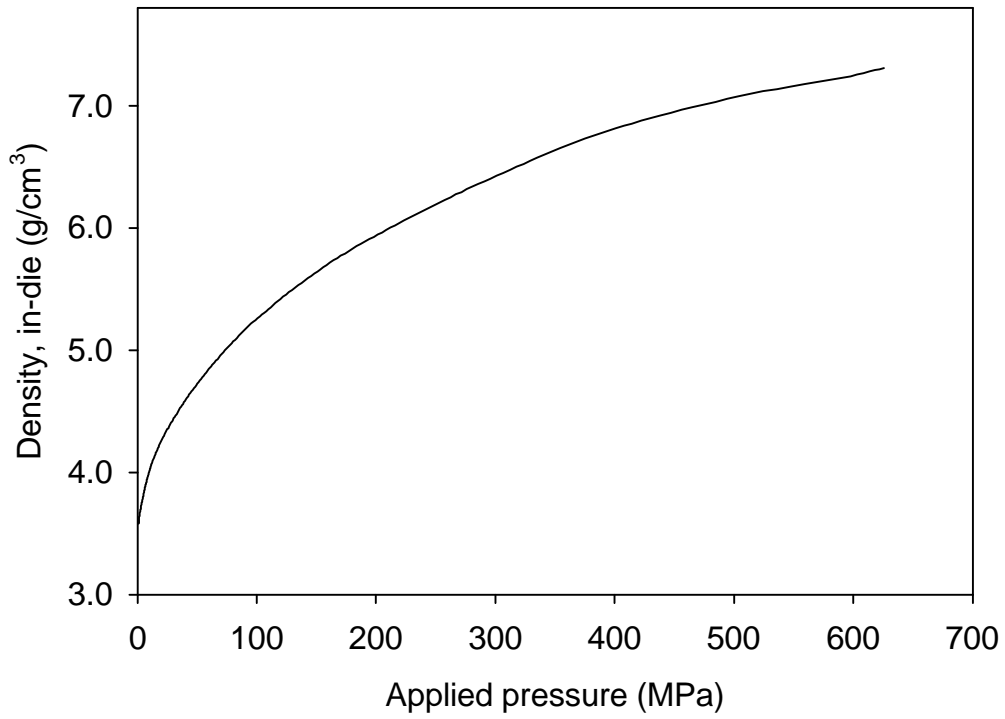


Figure 2: Effect of compacting pressure on the density of transverse rupture bars pressed at 55°C from the press-ready composite powder mix.

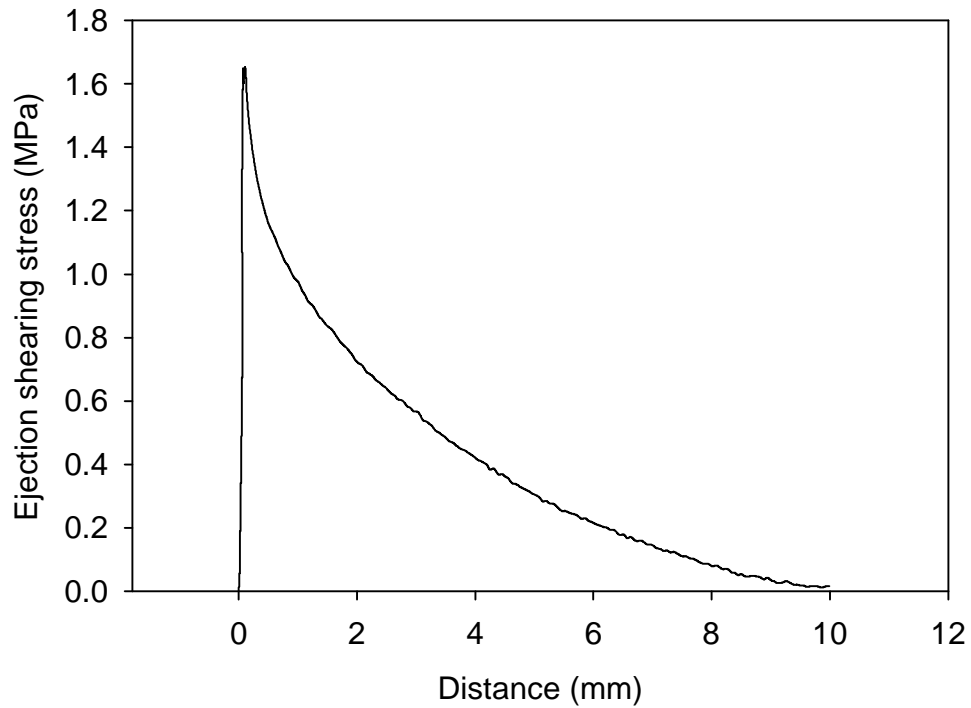
The compressibility curve presented in Figure 3a refers to the “in die density” of a small cylinder while the standard compressibility curve of Figure 2 refers to the “out-die density” of TR bars. The two curves correlate well. At a compacting pressure of 600 MPa, 7.18 g/cm³ out-die density was obtained with the TR bars (97.6% of theoretical density) and 7.24 g/cm³ in-die with the cylindrical specimens (98.4% of theoretical density). The difference between these densities may be associated with the springback that takes place during ejection and differences in specimen geometry and compaction conditions. Calculations showed that in this particular case, the major contribution came from the springback during ejection. A stripping pressure of about 23 MPa (1.65 tsi) is typically obtained on the cylinders with a sliding pressure that decreases smoothly as the part exits the die (Figure 3b).

The effect of density on the electrical resistivity before and after a thermal treatment at 325°C in air is presented in Figure 4. The resistivity is not significantly affected by the density in the interval studied in this work. This holds true for both green and heat-treated specimens. As expected, the electrical resistivity decreases during the thermal treatment, typically from 150 μΩ-m in the as-pressed state to 60 μΩ-m after the heat treatment. The resistivity values after the thermal treatment are relatively high and adequate for applications at low frequency, particularly in small components. In applications requiring higher electrical resistivities, the resistivity may be adjusted by varying the lubricating dielectric content or the thermal treatment conditions [3,4].

The effect of density on the mechanical strength of transverse rupture bars after thermal treatment and resin impregnation is presented in Figure 5. The mechanical strength of heat-treated bars increases with density and values around 120 MPa (18,000 psi) are obtained for specimens pressed to 7.20 g/cm³. The resin impregnation has no effect on high density specimens but a very beneficial impact on low density specimens is observed, e.g., a 60% increase in strength for bars pressed to 6.8 g/cm³. With this material system, it is thus possible to achieve mechanical strengths higher than 100 MPa (15,000 psi) by increasing the pressed density or by using resin impregnation.



a)



b)

Figure 3. Compressibility and ejection characteristics obtained for cylindrical specimens 9.5 mm in diameter by 8 mm thick pressed at 45°C using an instrumented die: a) in-die density as a function of the applied pressure and b) typical ejection curve.

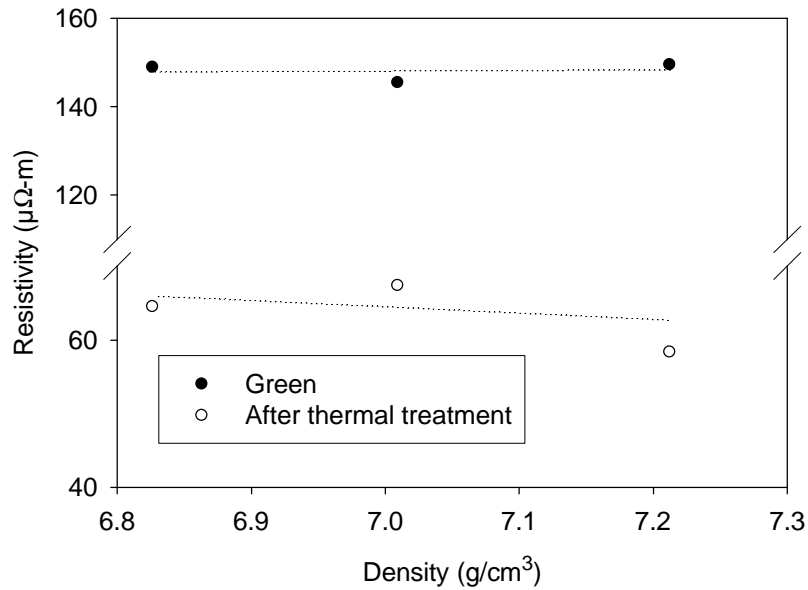


Figure 4. Effect of density on the electrical resistivity of transverse rupture bars before and after a thermal treatment at 325°C.

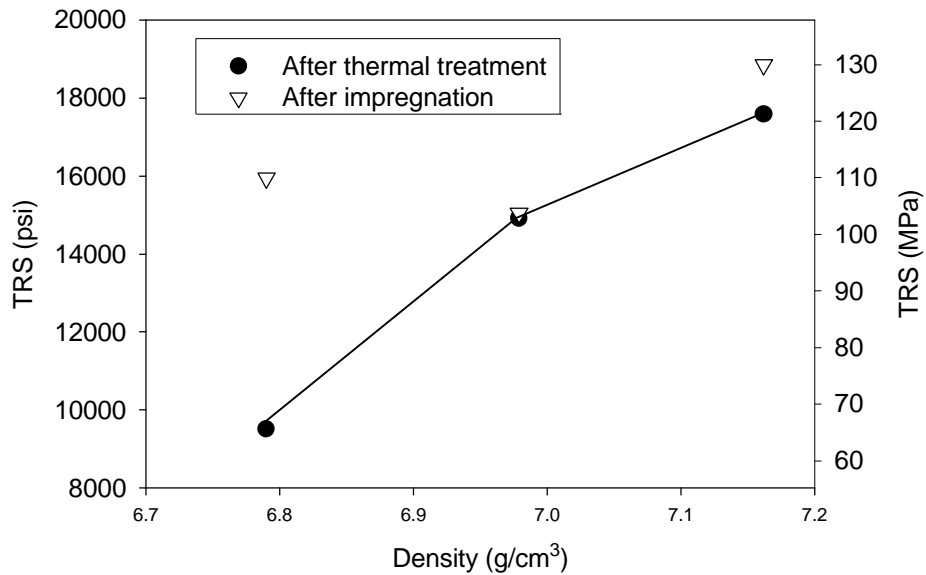


Figure 5. Effect of density on the transverse rupture strength after a thermal treatment at 325°C and after resin impregnation.

The DC magnetization curves for rings pressed to 6.8 g/cm³ and 7.2 g/cm³ are plotted in Figure 6. At a density of 7.20 g/cm³, a magnetic induction around 1.4 Tesla is achieved at an applied field of 11,940 A/m (150 Oe). Reducing the density shears the magnetization curve and reduces the induction

at a given applied field H and consequently lowers the permeability of the material. The shearing is associated with the increased thickness of the distributed air-gap (non magnetic interface between the iron particles) in the material when the density decreases. The effect of density on the DC magnetic properties is presented in Figure 7. The maximum permeability and maximum induction increase significantly with the density while the coercive force H_c decreases slightly. In fact, by increasing the density from 6.8 g/cm^3 up to 7.2 g/cm^3 , the maximum permeability increases by 39%, the maximum induction by 24% and the coercive force decreases by 4%.

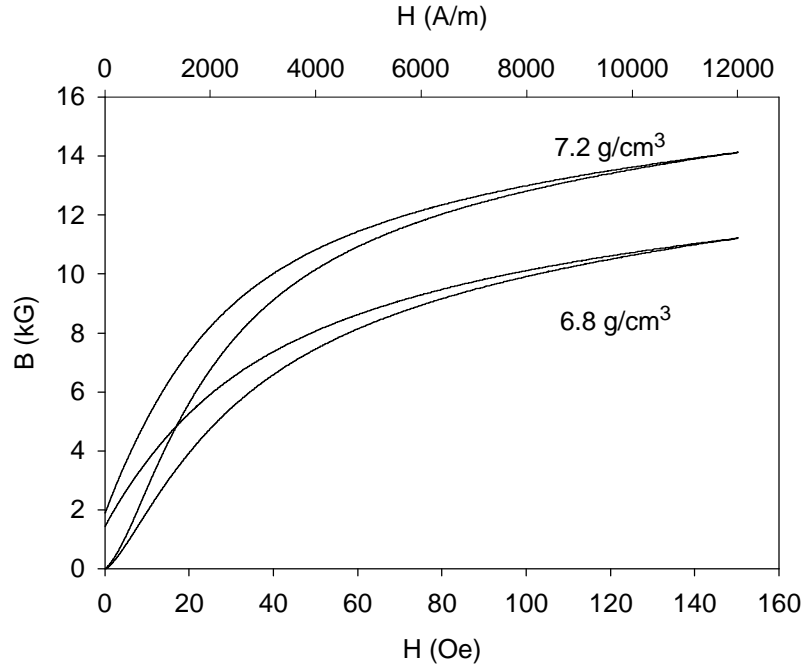
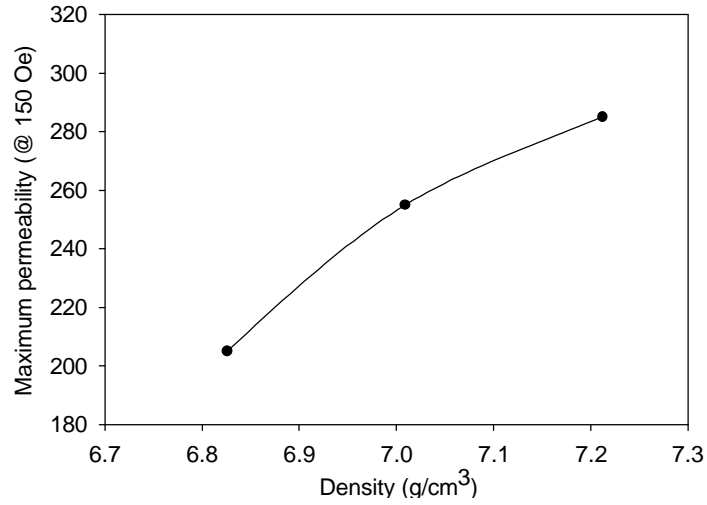


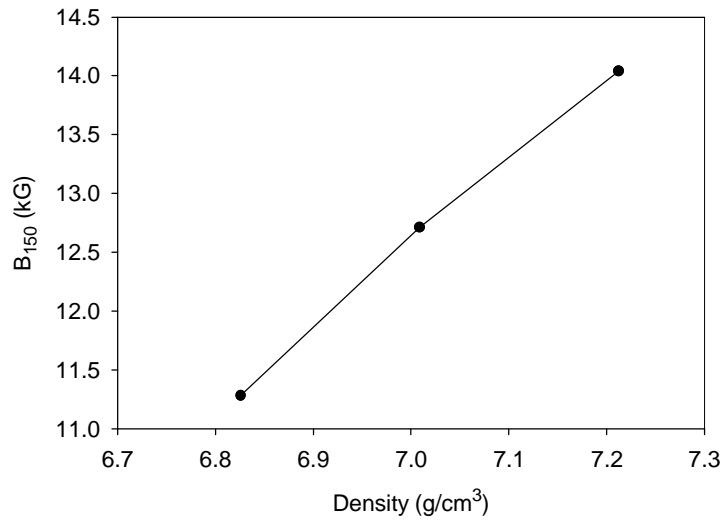
Figure 6. Effect of density on the DC magnetization curve measured at an applied field of 11,940 A/m (150 Oe).

The effect of density on the AC losses at 1 Tesla measured at 60 Hz and 400 Hz is presented in Figure 8. An increase in density from 6.8 g/cm^3 to 7.2 g/cm^3 decreases the total core loss at 1 Tesla from 10.8 W/kg to 9.1 W/kg at 60 Hz and from 80.2 W/kg to 65.3 W/kg at 400 Hz. This represents a decrease of about 18% in AC losses. This reduction must be mainly associated with the decrease of the hysteresis loss. The improvements in DC characteristics that occur when density increases have a beneficial effect on the hysteresis portion of the core loss. This also suggests that eddy-currents remain low and the electrical resistivity of the material is sufficiently high to prevent loss even at higher densities.

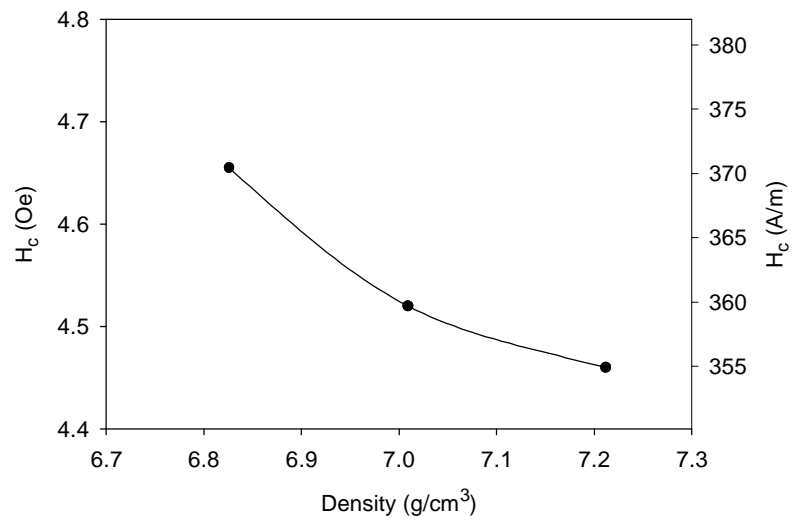
As shown, the density has a significant effect on both mechanical and magnetic properties and thus has to be considered when designing a P/M soft magnetic component. For instance, in certain applications, it may be found that density gradients affect the performance of the components and local distribution of densities may need to be considered. This non-uniform density distribution in pressed parts is a phenomenon well known by P/M metallurgists but generally neglected by electric machine designers that are used to homogeneous materials such as steel laminations. However, a good lubrication during compaction and optimized press settings usually minimize density gradients in pressed parts.



a)



b)



c)

Figure 7. Effect of density on DC magnetic properties: a) maximum permeability; b) induction at an applied field of 11,940 A/m and c) coercive force.

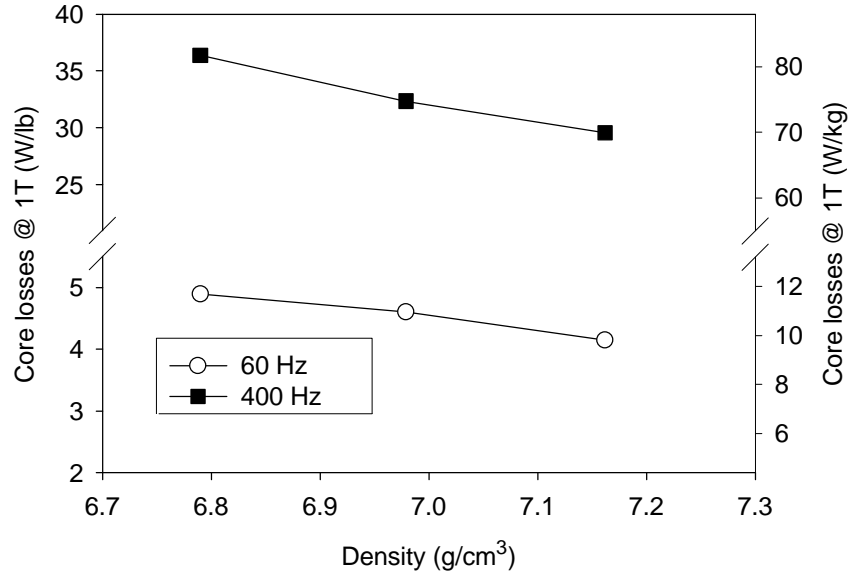


Figure 8: Effect of density on the core losses at 1 T measured at 60 and 400 Hz.

3.2 Compaction of the composite powder mix on an industrial press.

The density of the 20 mm thick stator segments as a function of the compacting pressure is presented in Figure 9. Density values are slightly lower than those predicted by the compressibility curve of Figure 2. At 480 MPa for example, density values of 7.06 g/cm³ and 7.01 g/cm³ were obtained for the TR bars and the stator segments respectively. This difference is attributed to the shape of the specimens. The segments are thicker than the TR bars (20 mm versus 6.35 mm) and the friction surface area is much larger (54.3 cm² versus 2.2 cm²). This friction between the surface of the part and the die walls causes a pressure drop along the part height and consequently affects the density of the specimens. As mentioned earlier, this may affect the magnetic properties of the soft magnetic composites, especially the permeability and the magnetic induction.

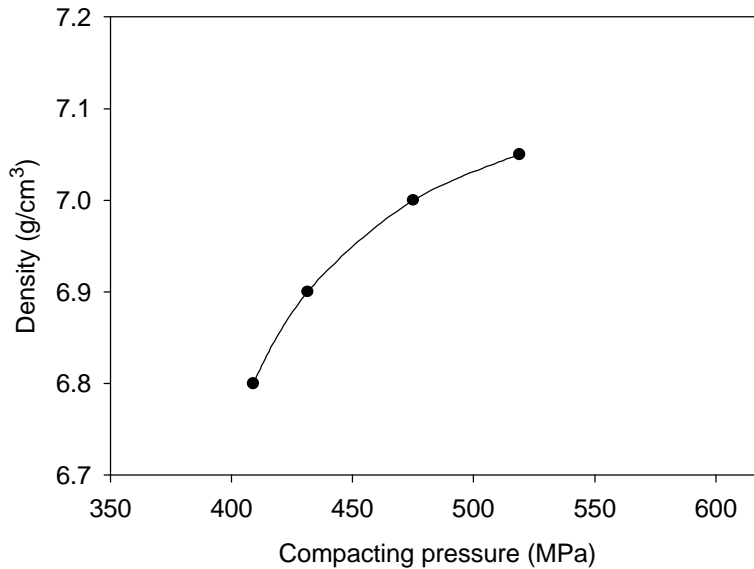


Figure 9. Effect of compaction pressure on the density of the 20 mm thick stator segments.

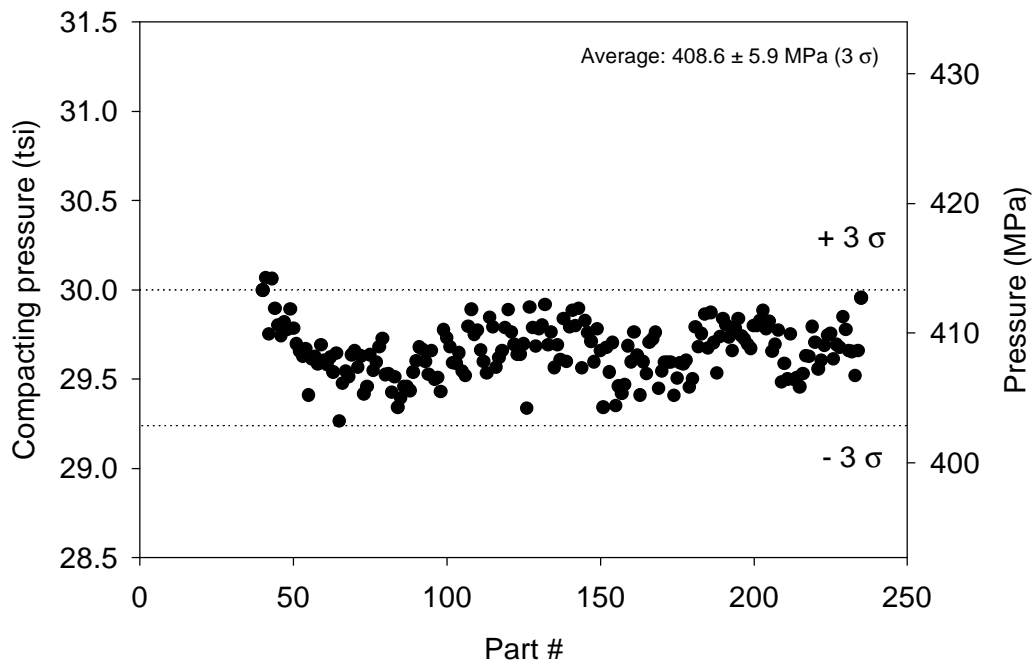
Variations in compaction pressure and part weight during the production of a short series of 20 mm thick segments are plotted in Figure 10. The lines above and below the plots represent the plus and minus 3 sigma values. The stators were pressed at a green density of about 6.85 g/cm³ at an average compaction pressure of 408.6 MPa (29.7 tsi) with a total variation of 11.4 MPa or 2.8% (6 sigma). A total variation of 0.6% (6 sigma) was obtained for the weight that is rather small, indicating that the process was stable and the powder flowability as well as the press operating conditions were adequate for this relatively complex part geometry.

Typical ejection curves for segments of different thicknesses and densities are reported in Figure 11. The actual maximum force needed to eject a part increases almost linearly with the part thickness, but the ejection pressure (force divided by the sliding surface area of the component) does not. This is illustrated in Figure 11a showing that the stripping pressure does not increase with the part thickness.

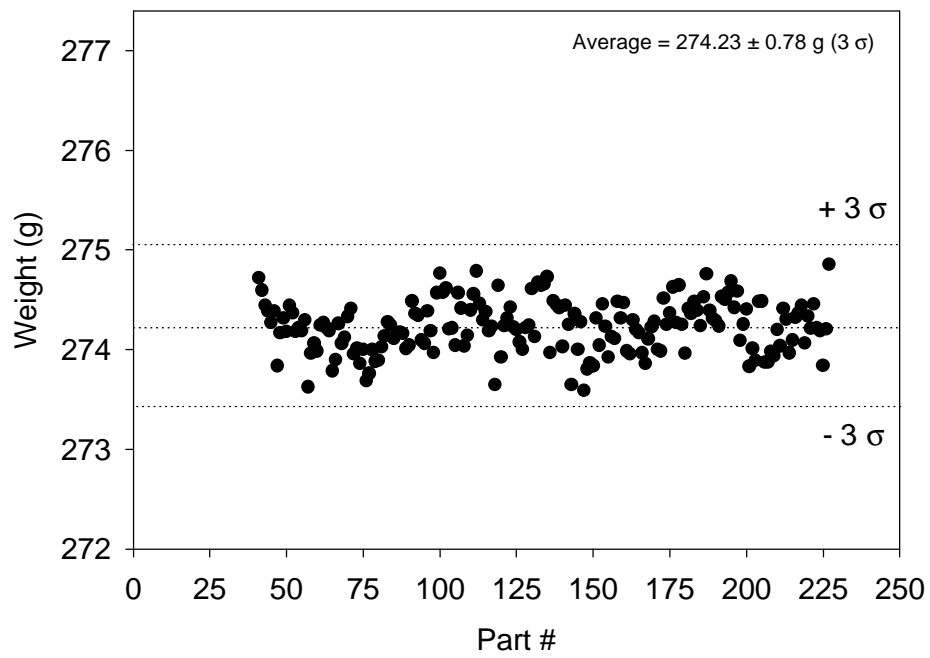
Considering that a higher die fill is required for thicker parts, the sliding distance during ejection increases with part thickness. Consequently, the area under the ejection curve that represents the energy needed to eject the part from the die increases. This is particularly evident for the 25 mm thick segments. It appears that the lubricating film between the compacted specimen and the die walls may be modified during the ejection or affected by the sliding distance. In the present case, the sliding ejection pressures for the 15 and 20 mm thick segments are similar and slightly lower than those of the 25 mm thick segments.

Figure 11b, presenting ejection curves for 20 mm thick segments, shows that the stripping pressure and ejection energy increase when the compacting pressure and density of the segments increase. This is partly due to the fact that the radial pressure increases when the compaction pressure increases. In addition, the die fill as well as the sliding distance increase with the density. This affects the ejection energy of the specimens.

In general, for the material, part geometry, die and processing conditions used during these trials, the lubricating characteristics were adequate at all thicknesses and densities studied. It is worth mentioning that the ejection characteristics were also very stable all along the short production runs.



a)



b)

Figure 10. Variation in a) compaction pressure and b) part weight during the production of the 20 mm stator segments.

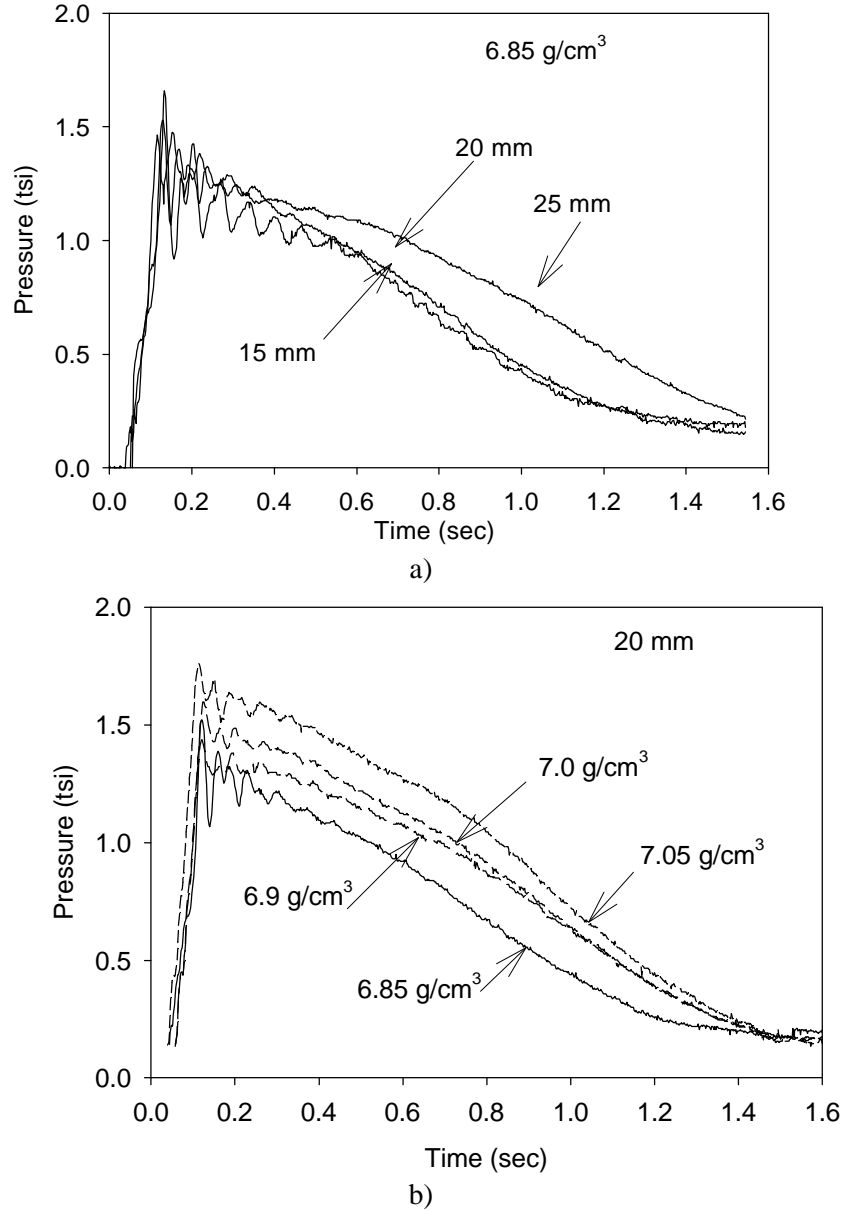


Figure 11. Typical ejection curves for the stator segments: a) for different thicknesses at a fixed density of 6.85 g/cm³ and b) for different densities at a fixed thickness of 20 mm.

4. CONCLUSION

In this study, the properties and compaction-ejection characteristics of a new press-ready mix intended for AC magnetic applications at low frequency (50-60 Hz) were investigated. Trials were carried out in laboratory as well as on an industrial press for the compaction of stator segments of an electric DC motor.

This new ferromagnetic powder mix was processed by conventional compaction followed by a thermal treatment at 325°C. With this high compressibility powder mix, green densities in the 7.20 g/cm³ range were achieved at a compacting pressure of 620 MPa (45 tsi). The compacting pressure or density has a significant effect on most of the mechanical and magnetic properties. For instance, the mechanical strength, the permeability and magnetic induction increase with density while core losses

at 60 Hz and 400 Hz decrease. Regarding the strength, TRS values higher than 100 MPa (15,000 psi) were obtained by increasing the density or by using resin impregnation. Besides, the electrical resistivity was not significantly affected by the density. A relatively high value of 60 $\mu\Omega\cdot\text{m}$ was obtained, which is effective for applications at low frequency, particularly in small components.

This mix was successfully compacted into complex parts on an industrial press. Rotor segments of different thicknesses (15 to 25 mm) and densities (6.85 to 7.05 g/cm³) were pressed. Good compaction and ejection behavior were observed. The stability of the compacting pressure, ejection pressure and part weight was also demonstrated for short production runs.

ACKNOWLEDGEMENTS

The authors greatly acknowledge Mr. J.Y. Dubé of EPS (Energy Propulsion System) for his contribution to this work. From IMI, the authors also acknowledge Mr. G. St-Amand for his help in the experimental work and Dr. Y. Thomas for the helpful discussions on the lubrication and the compaction/ejection characteristics.

REFERENCES

¹ L.P. Lefebvre and C. Gélinas, “Effect of Material Insulation and Part Geometry on the AC Magnetic Performances of P/M Soft Magnetic Composites”, *Advances in Powder Metallurgy and Particulate Materials* - 2001, Vol. 7, MPIF, Princeton, NJ, pp 36-50.

² L.P. Lefebvre, S. Pelletier, B. Champagne and C. Gélinas, “Effect of Resin Content and Iron Powder Particle Size on Properties of Dielectromagnetics”, *Advances in Powder Metallurgy & Particulate Materials* - 1996, Vol. 6, MPIF, Princeton, NJ, pp 20-47 to 20-61.

³ L.P. Lefebvre, S. Pelletier, Y. Thomas and C. Gélinas, “Iron Compacts for Low Frequency AC Magnetic Applications : Effect of Lubricants”, *Advances in Powder Metallurgy & Particulate Materials* - 1998, Vol. 2, MPIF, Princeton, NJ, pp 8-61 to 8-73.

⁴ L.P. Lefebvre, S. Pelletier and C. Gélinas, “Iron Compact for Low Frequency AC Magnetic Applications : Effect of Thermal Treatments”, *Advances in Powder Metallurgy & Particulate Materials* - 1998, Vol. 2, MPIF, Princeton, NJ, pp 8-47 to 8-59.